
GITA: Graph to Visual and Textual Integration for Vision-Language Graph Reasoning

Project Page: v-graph.github.io

Yanbin Wei^{1,2*}, Shuai Fu^{1,3*}, Weisen Jiang^{1,2}, Zejian Zhang⁴, Zhixiong Zeng⁴,
Qi Wu³, James T. Kwok², Yu Zhang^{1,†}

¹Department of Computer Science and Engineering, Southern University of Science and Technology

²Department of Computer Science and Engineering, Hong Kong University of Science and Technology

³Australia Institute of Machine Learning, University of Adelaide

⁴Tencent

{yanbin.ust, fus.jayce, waysonkong, zejianshang33, yu.zhang.ust}@gmail.com
barretzeng@tencent.com
qi.wu01@adelaide.edu.au
jamesk@cse.ust.hk

Abstract

Large Language Models (LLMs) are increasingly used for various tasks with graph structures. Though LLMs can process graph information in a textual format, they overlook the rich vision modality, which is an intuitive way for humans to comprehend structural information and conduct general graph reasoning. The potential benefits and capabilities of representing graph structures as visual images (i.e., *visual graph*) are still unexplored. To fill the gap, we innovatively propose an end-to-end framework, called **Graph to vIsual and Textual IntegrAtion** (GITA), which firstly incorporates visual graphs into general graph reasoning. Besides, we establish **Graph-based Vision-Language Question Answering** (GVLQA) dataset from existing graph data, which is the first vision-language dataset for general graph reasoning purposes. Extensive experiments on the GVLQA dataset and five real-world datasets show that GITA outperforms mainstream LLMs in terms of general graph reasoning capabilities. Moreover, We highlight the effectiveness of the layout augmentation on visual graphs and pretraining on the GVLQA dataset.

1 Introduction

Graph reasoning tasks are pivotal in domains such as recommendation systems (He et al., 2020; Wang et al., 2021), social network analysis (Cao et al., 2020; Huang et al., 2021), and knowledge graph reasoning (Zhang et al., 2021; Liu et al., 2022). Various architectures have been developed, from shallow embedding methods (Bordes et al., 2013; Socher et al., 2013) to advanced Graph Neural Networks (GNNs) (Kipf & Welling, 2016; Xu et al., 2018) and graph Transformers (Zhang et al., 2020; Kreuzer et al., 2021; Chen et al., 2022). While these models excel in graph reasoning tasks, they often lack generalizability, flexibility, and user-friendliness. Firstly, achieving good performance with these models typically requires domain-specific tuning, which limits their abilities to generalize across different domains. Additionally, these models struggle to handle diverse tasks with the same architecture. Each task often requires a specialized design, including task-specific data processing

*Equal contribution.

†Corresponding author.

and decoders, leading to limited flexibility. Lastly, compared to the Large Language Models (LLMs) that can engage in conversations with users, these models are less user-friendly.

In contrast, LLMs have shown exceptional generalization capabilities across a diverse spectrum of reasoning tasks (Wei et al., 2022; Yu et al., 2024; Zhou et al., 2023) by encapsulating task-specific demands within a cohesive and interpretable mechanism - text prompts, under a unified architecture with minimal domain-specific adjustments. Those advantages have sparked investigations into the potential of LLMs for graph reasoning. Recent developments lend credence to the notion that LLMs can indeed interpret and manipulate graph-structured data through textual representations. For example, InstructGLM (Ye et al., 2023), GPT4Graph (Guo et al., 2023), and LLMtoGraph (Liu & Wu, 2023) convert graphs into textual descriptions and then use those descriptions paired with queries to enable LLMs to generate accurate responses for graph reasoning tasks. Furthermore, the introduction of benchmarks such as GraphQA (Fatemi et al., 2024) and NLGraph (Wang et al., 2023) is a testament to the growing interest in evaluating LLMs’ effectiveness on graph reasoning tasks framed in natural languages.

Despite the development of numerous methods and benchmarks for graph reasoning on LLMs, they often overlook the valuable vision modality, which however is a natural means for humans to comprehend structural information and has demonstrated its success in various visual reasoning scenarios Hudson & Manning (2019); Zellers et al. (2019); Zhang et al. (2019); Johnson et al. (2017); Andreas et al. (2016); Suhr et al. (2019). Consequently, the following questions arise: (1) *Can incorporating visual information be beneficial for general graph reasoning scenarios?* (2) *If so, how can we effectively integrate the vision modality into graph reasoning?* To the best of our knowledge, these questions remain unexplored.

To answer them, we first propose an end-to-end framework called **Graph to vIsual and Textual IntegrAtion (GITA)** that systematically integrates visual information into instruction-based graph reasoning, by rendering graph structures to customized visual images which are called *visual graph*. Specifically, the GITA framework has four components: a graph visualizer for generating visual graphs, a graph describer for producing textual descriptions of the graph structure, a task-based questioner that organizes the description and requirements of the current task into prompt instruction, and a Vision-Language Model (VLM) to perform vision-language graph reasoning. According to the proposed GITA framework, visual information can be incorporated into many tasks with explicit or implicit graph structures, without sacrificing its versatility, flexibility, or user-friendliness. Besides, since there is no dataset for vision-supported general graph reasoning capabilities, we establish the first vision-language dataset for general graph reasoning purposes called **Graph-based Vision-Language Question Answering (GVLQA)** based on the proposed GITA framework. The GVLQA dataset consists of 526K instances covering seven representative graph reasoning tasks, aiming to thoroughly evaluate the structure-based graph reasoning abilities of VLMs and LLMs. Extensive experiments on the GVLQA dataset and five real-world datasets demonstrate the effectiveness of the proposed GITA model. Furthermore, we delve into the effects of visual graph augmentation strategies and find that layout augmentation can dramatically boost vision-based graph reasoning performance.

Our main contributions are summarized as follows.

- We introduce an end-to-end GITA framework, innovatively integrating vision modality to boost the graph reasoning abilities of language models.
- We establish GVLQA, the first vision-language question-answering dataset for general graph reasoning purposes. It can be used to thoroughly evaluate the structure-based graph reasoning abilities of LLMs/VLMs and can also be used as pretraining data to boost the performance of downstream tasks.
- Extensive experiments on benchmark datasets across various graph reasoning tasks demonstrate the effectiveness of the proposed GITA framework, and highlight the benefits of layout augmentation on visual graphs.

2 Related Work

Graph Reasoning. Graph reasoning (Battaglia et al., 2018; Wu et al., 2020) aims to answer questions based on graphs, which involves utilizing graph structures to guide the reasoning process to generate answers. Graph reasoning has a wide variety of applications in social network analysis (Newman,

2003; Leskovec et al., 2008), bioinformatics (Jeong et al., 2001; Gavin et al., 2006), chemistry (Gilmer et al., 2017), physics (Battaglia et al., 2016), knowledge graph reasoning (Bordes et al., 2013), and recommendation systems (Koren et al., 2009; He et al., 2017). Many graph reasoning methods have been proposed. Early attempts Bordes et al. (2013); Socher et al. (2013) learn node and edge representations through shallow modules, which may have only limited expressive power. Graph Neural Networks (GNNs) such as GCN Kipf & Welling (2016), GAT Velickovic et al. (2017), GraphSAGE Hamilton et al. (2017), MPNN Gilmer et al. (2017), and GIN Xu et al. (2018) use message-passing paradigm Gilmer et al. (2017) to model graph dependencies and update node features. Transformer-based graph models Zhang et al. (2020); Kreuzer et al. (2021); Chen et al. (2022) further propose to use self-attention to increase the expressiveness and long-range dependency. However, as discussed in Sec 1, these models may exhibit limited generalizability, flexibility, and user-friendliness.

LLMs on Graph Reasoning. There have been many attempts to use LLMs in graph reasoning. Depending on how they align the input spaces of graphs and LLMs, we categorize them into two types: Graph-to-text and Graph-to-token. Graph-to-text methods transform a graph into textual descriptions, which are concatenated with the instructions and fed to the LLM for querying. For example, InstructGLM (Ye et al., 2023) uses natural language to describe the graph and proposes instruction prompts to fine-tune the LLM. He et.al He et al. (2024) applies LLMs to explain graphs for training GNNs, while Chen et.al Chen et al. (2023) treat LLMs as enhancers to exploit text attributes or as predictors for node classification on text-attributed graphs. GPT4Graph (Guo et al., 2023) and LLMtoGraph (Liu & Wu, 2023) convert graphs into specific code or natural language formats by the powerful ChatGPT (OpenAI, 2022, 2023). On the other hand, Graph-to-token methods include GraphGPT (Tang et al., 2023), GraphToken (Perozzi et al., 2024) and LLaGA (Chen et al., 2024). For these methods, the graph is represented as a specially designed token sequence, which is projected or merged into the LLM’s token space for text-based reasoning. However, none of the aforementioned methods represent the graph structure information as images, highlighting the uniqueness of the proposed GITA framework and GVLQA dataset.

Large Vision-Language Models. Large VLMs have significantly expanded the cognitive abilities of LLMs by integrating the vision modality to address vision-language tasks. Many methods have been proposed. Some early explorations like Flamingo Alayrac et al. (2022), CLIP Radford et al. (2021), and BLIP-2 Li et al. (2023) use a visual encoder for processing images and align the visual and textual embeddings. Subsequent models like LLaVA Liu et al. (2023) and MiniGPT-4 Zhu et al. (2023) combine visual and textual inputs in a single LLM for solving multimodal tasks. InstructBlip Dai et al. (2023) proposes an instruction-aware query transformer and trains a vision-language model by instruction tuning. However, despite progress in a wide range of vision-language tasks (Zhang et al., 2024), using visual information in graph reasoning remains overlooked. We take the first step in this field, pushing the boundaries of VLMs in graph reasoning.

3 GITA: Graph to Visual and Textual Integration

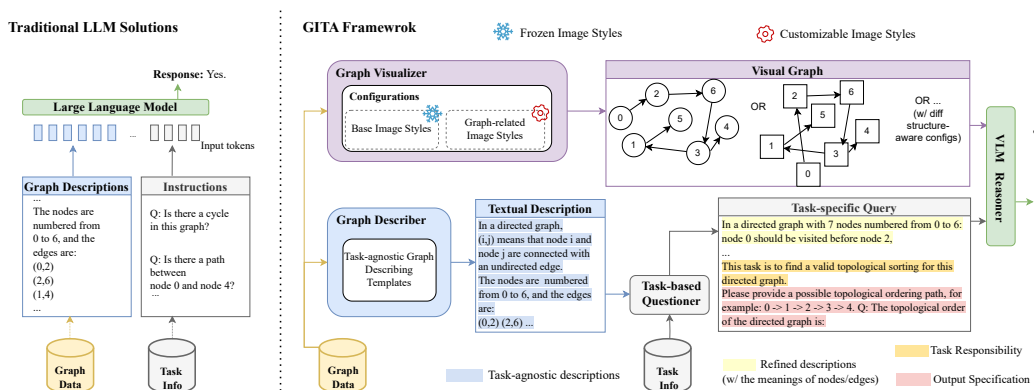


Figure 1: The architecture of the GITA framework with comparison to existing LLM solution.

3.1 Preliminary

Graph Reasoning. In traditional graph reasoning settings, models typically rely on two main inputs: i. the graph structure $G = \{C, E\}$, where C and E are the set of vertices and edges, respectively; ii. the task requirement T , encompassing specific operations or questions pertaining to the graph. Based on the information provided in G and a specific task requirement T , models are expected to output a reasonable answer A . On the other hand, in the context of instruction-based graph reasoning methods, it is necessary to convert these inputs into textual form. This transformation facilitates graph reasoning within natural language, allowing for improved interpretation and harnessing the formidable reasoning capabilities of large language models.

3.2 Architecture

Overview. Different from the above graph reasoning methods, we propose a **Graph to Image-Txt Assistant (GITA)**, which is the first attempt to perform graph reasoning in a vision-text-based manner. GITA comprises four pivotal components: a task-agnostic graph visualizer V , a graph describer D , a task-specific questioner Q , and a VLM reasoner R_ϕ , as illustrated in Figure 1. Firstly, V and G are designed to produce visual depictions (i.e., *visual graphs*) and textual descriptions of the graph structure inputs, respectively. Then, given the task requirement T and the textual description produced by D , Q is designed to formulate a task-specific query. Finally, R_ϕ receives the visual graph from V and the task-specific query from Q as the visual input I_G and textual input Q_G^T , respectively, consequently generating answers A in natural language.

Graph Visualizer. The role of the graph visualizer is to generate visual graphs from structural graphs. Representing a structural graph with an image is not unique, as there can be variations in many aspects, such as backdrop colors, layouts, and node shapes. These variations may enhance the robustness of models through effective training but simultaneously increase the learning difficulty for models. Therefore, a careful trade-off between *consistency* and *variety* is necessary during the graph visualization process. This trade-off is reflected in our design of graph visualizer, by maintaining consistency in basic image styles common to general images (i.e., size, resolution, backdrop, etc.) and only introducing customizable variations in four graph-related image styles unique to visual graphs (i.e., layout, node shapes, node outline styles, and edge thickness). Hence, the graph visualization of V can be concisely encapsulated by the following equation:

$$I_G = V(G, \Gamma, \Delta), \tag{1}$$

where I_G denotes the visual graph derived from graph G , while Γ and Δ are the fixed basic image styles and customizable graph-related image styles, respectively.

Besides, visualizing the entire graph can be challenging when the number of nodes or edges is very large, affecting the clarity of the images. To address this, our graph visualizer adopts a typical strategy of k -hop subgraph sampling. Specifically, k -hop subgraph sampling for a node u in the set of vertices C involves selecting a subgraph $G_u = \{C_u \subseteq N_k(u), E_u \subseteq E\}$, where $N_k(u)$ includes nodes within k steps from u and each edge (i, j) in E_u connects nodes within C_u . To generate the visual graph of the k -hop subgraph G_u centered on u , the nodes within G_u will be relabeled from 0 to $|C_u| - 1$ to facilitate the generalization of visual graphs. Subsequently, this relabeled subgraph G_u is input into the graph visualizer to generate its the visual graph I_{G_u} as shown in Eq. 1.

In practice, the graph visualizer can be implemented by a variety of graphic visualization tools, such as Graphviz (Gansner & North, 2000), Matplotlib (Tosi, 2009), and NetworkX (Hagberg et al., 2008). Among them, Graphviz can automatically design the layouts of visual graphs, especially suitable for building large-scale datasets. Matplotlib is excellent for customizable plots with fine-grained control, and NetworkX excels in complex network analysis. We have implemented various graph visualizers using modular, plug-in architecture in GITA. Specific examples of the visual graphs generated with these tools can be found in Appendix C.

Graph Describer. The graph describer D is tasked with generating task-agnostic textual descriptions of a given graph G . To ensure the clarity and fidelity of these descriptions, we meticulously craft a curated set of *graph-describing templates*. The graph description templates outlined in Appendix D are designed to cover a broad spectrum of scenarios, accommodating various graph configurations including directed or undirected graphs and those with or without node or edge weights. To generate a specific description for a given graph, the graph describer initially selects the appropriate

template based on the graph’s characteristics, such as its directionality and whether it includes node attributes or edge weights. Subsequently, this template is used by replacing placeholders with actual data, such as the number of nodes, the number of edges, and the endpoints of each edge, to craft detailed descriptions tailored to the specific graph in question. The process for D to generate textual descriptions can be formulated as follows:

$$D_G = D(G, P), \quad (2)$$

where D_G denotes the textual description generated by graph describer, and P is the graph-describing template of the graph G .

By introducing these unified and structured graph-describing templates, the graph describer is empowered to generate coherent and informative descriptions that focus on the inherent characteristics of the graph itself, independent of specific task requirements.

Questioner. The questioner Q , is tailored to capture the intricate requirements of specific tasks and reflect them in its output task-specific query. In detail, Q receives the task-agnostic textual descriptions from the graph describer and refines them to align with the task context by elucidating the concrete meanings of nodes and edges. These refined descriptions are then enriched with task responsibilities and input/output specifications to form task-specific queries. The formulation of the questioner to generate the task-specific queries can be represented as follows:

$$Q_G^T = Q(T, D_G), \quad (3)$$

where Q_G^T represents the task-specific query generated by the questioner with given the task requirement T and the textual description D_G . The construction of task-specific queries can be approached in two main ways: manual-template-based constructing and bootstrapping LLM agents. manual-template-based constructing enriches D_G with task-specific manual templates, which is preferred for tasks with precise requirements, such as the Traveling Salesman Problem (TSP) (Dantzig et al., 1954), where accuracy is critical and the task definitions are well-understood. This is because it can ensure clarity and reduces the risk of errors due to its meticulous attention to detail. On the other hand, bootstrapping LLM agents for automated synthesis is more economic and suitable for dynamic or bespoke tasks, such as robotic planning or complex gaming scenarios, as it can take advantage of the speed and adaptability of LLM agents to interpret context and generate appropriate queries, minimizing manual effort and enhancing responsiveness to changing conditions. Both methods are illustrated with examples in Appendix E, showcasing their applications and benefits in different scenarios.

VLM Reasoner. The VLM reasoner R_ϕ is to perform the final graph reasoning with visual inputs I_G from V and textual inputs Q_G^T from Q , consequently outputting responses in natural languages. This reasoning process can be presented as the following formula:

$$A = R(I_G, Q_G^T), \quad (4)$$

where A is the answer generated by a vision-language model R . In this work, we specifically adopt GPT-4V and LLaVA-7B/13B as VLM reasoners. Those models are regarded as representatives in the realm of closed-source and open-source VLMs, respectively.

In summary, GITA systematically incorporates the vision modality into instruction-based graph reasoning. In Appendix A, we discuss the characteristics of GITA, in aspects of generalizability, flexibility, user-friendliness, and large-graph scalability.

3.3 Visual Graph Augmentation

Visual graphs generated for the same graph G can be considered as a unique data augmentation technique. Building on the four graph-related image styles introduced in the graph visualizer part of Sec 3.2, we propose the following corresponding augmentation strategies: **layout augmentation**, **node shape augmentation**, **node outline style augmentation**, and **edge thickness augmentation**. Specifically, layout augmentation involves altering the layout styles while keeping all other settings constant. Similarly, by changing only the respective attributes, we can implement node shape augmentation, node outline style augmentation, and edge thickness augmentation. These four proposed augmentation strategies can facilitate studies on the importance of each in enhancing the graph reasoning abilities of VLM reasoners.

3.4 Training

Given a visual graph I_G and a text-specific query Q_G^T , along with the target answer A_t , the VLM reasoner of GITA is trained to generate answers A . Specifically, I_G is input into the vision encoder of the VLM reasoner, resulting in a set of visual features F . If there is a dimension difference between F_v and the pretrained word embeddings, these F will be aligned with the pretrained word embedding space of the text decoder by a vision-to-text projector. Finally, the aligned visual features $F_{aligned}$ and Q_G^T are concatenated as input sequences of the text decoder.

Formally, given I_G , Q_G^T , and A_t , the VLM reasoner is trained by minimizing the negative log-likelihood as follows:

$$\mathcal{L}_\phi = - \sum_{i=1}^{|A|} \log p_\phi(A_i | F_{aligned}, Q_G^T, A_{<i}), \quad (5)$$

where ϕ is trainable parameters and A_i denotes the prediction token at the i -th position. Besides, $A_{<i}$ represents the first $i - 1$ predicted tokens. During the inference process, GITA is capable of accepting structure graphs as inputs and performing graph reasoning in an end-to-end manner.

4 GVLQA Dataset

In this section, we introduce the GVLQA dataset to fill the absence of a vision-language-based general graph reasoning dataset. It is designed to: 1) evaluate the graph reasoning capabilities of VLMs or LLMs; 2) help models acquire fundamental graph comprehension and reasoning abilities as a pretraining dataset.

4.1 Construction

The GVLQA dataset is created by utilizing the graph visualizer, the graph describer, and the questioner in GITA to generate vision-language-based question-answer pairs for graph reasoning on an open-source graph dataset. Specifically, we first extract both the original graph structures and the ground-truth outputs from the NLGraph-full dataset (Wang et al., 2023). Then the graph visualizer (detailed in Sec 3.2) and the graph describer (outlined in Sec 3.2) are used to generate visual graphs and textual descriptions for these original graph structures, respectively. Afterward, the questioner (described in Sec 3.2) further improves and enriches the textual descriptions by converting them into textual queries. At the same time, it transforms the ground-truth output into text-based answers, following specific output requirements. By combining these visual graphs, textual queries, and text-based answers, we obtain the Graph-based Vision-Language Question Answering (GVLQA) dataset.

In the process of establishing GVLQA, we employed graphviz (Gansner & North, 2000) to instantiate the graph visualizer. This choice is made due to its multitude of pre-defined layout algorithms, which enable convenient adjustment of visual graph layouts. Additionally, manual-template-based constructed queries are utilized as the questioner because these tasks are famous with well-defined requirements.

4.2 Structure

The GVLQA dataset comprises 526K samples, each consisting of a visual graph, a textual query, and the corresponding answer. It is divided into five subsets: GVLQA-BASE, and four augmentation subsets GVLQA-AUGLY, GVLQA-AUGNS, GVLQA-AUGNO, and GVLQA-AUGET. In GVLQA-BASE, the visual graphs are uniformly styled. The remaining four augmentation subsets are derived from GVLQA-BASE through the four visual graph augmentations (Sec 3.3), varying in six different layouts, three node shapes, four node outline styles, and four degrees of edge thickness, respectively. Detailed statistics for each subset are presented in Table 4 in Appendix B.

Each GVLQA subset undergoes evaluation across seven graph reasoning tasks, outlined as follows.

- **Connectivity** (Sedgewick, 2001) (denoted by Connect): to determine whether two randomly selected nodes u and v in an undirected graph are connected.
- **Cycle** (Sedgewick, 2001): to identify whether a cycle exists in an undirected graph.

- **Topological Sort** (Kahn, 1962) (denoted by TS): to find a valid topological sorting for a directed acyclic graph. Here a topological sorting is to output a linear ordering of nodes such that for every directed edge $u \leftarrow v$, node u comes before v in the ordering.
- **Shortest Path** (Dijkstra, 1959) (denoted by SP): to find the shortest path between two nodes in a weighted undirected graph, where the shortest path between two nodes is the path connecting the two nodes with the minimum sum of edge weights along the path.
- **Maximum Flow** (Ford & Fulkerson, 1956) (denoted by MaxFlow): to calculate the maximum flow from a source node to a sink node in a network graph.
- **Bipartite Graph Matching** (Karp et al., 1990) (denoted by BGM): to find a matching set in a bipartite graph that has the largest number of edges, where a matching set is a collection of edges in which no two edges share any common node.
- **Hamilton Path** (Gould, 2003) (denoted by HP): to find a valid Hamilton path in an undirected graph, where a Hamiltonian path is a path that traverses each node in a graph exactly once.

Figure 6 offers illustrations for those tasks in the GVLQA-BASE dataset. Illustrations of all GVLQA subsets are provided in Appendix G.

5 Experiments

Table 1: Accuracy (%) comparisons on GVLQA-BASE under zero-shot and fine-tuning settings, where “VO” denotes a variant of GITA using only the vision modality.

Models	Connect	Cycle	TS	SP	MaxFlow	BGM	HP	Avg
<i>Zero-shot</i>								
LLaMA2-7B	50.06	49.43	0.00	0.00	0.00	0.00	0.00	14.21
Vicuna-7B	50.06	49.43	0.00	0.00	0.00	0.00	0.00	14.21
GITA-7B (VO)	50.06	50.33	0.00	0.00	0.00	0.00	0.00	14.34
GITA-7B	50.06	49.43	0.00	0.00	0.00	0.00	0.00	14.21
GPT-4 Turbo	76.70	49.51	19.59	35.35	6.89	42.11	47.04	39.60
GITA-ZS (VO)	57.76	63.34	5.34	4.88	1.59	46.60	10.74	27.18
GITA-ZS	82.58	51.46	19.71	37.69	6.00	52.21	50.00	42.81
<i>Fine-tuning</i>								
LLaMA2-7B	97.33	94.63	33.26	26.01	9.56	90.86	23.95	53.66
Vicuna-7B	97.58	95.04	34.46	25.98	9.33	91.04	25.55	54.15
GITA-7B (VO)	59.97	96.34	13.30	5.72	2.89	93.01	1.11	38.91
GITA-7B	98.95	96.67	41.12	32.15	20.00	93.19	29.26	58.76
LLaMA2-13B	98.79	93.36	33.83	27.93	12.22	91.34	33.46	55.85
Vicuna-13B	99.35	94.39	36.73	28.53	11.34	92.65	34.81	56.83
GITA-13B (VO)	58.00	96.91	14.45	5.72	4.89	93.19	1.85	39.29
GITA-13B	99.14	95.60	38.69	40.47	20.66	92.12	33.33	60.00

In this section, we extensively evaluate the performance of LLM baselines and the proposed GITA on the GVLQA-BASE and five real-world datasets. To better clarify the reasoning capabilities of solely visual graphs, we also test GITA without the textual descriptions of graphs, which can be considered as a variant of GITA and denoted as vision-only (VO). In this case, the visual graph is the only information source for graph reasoning. Additionally, we investigate the importance of visual graph augmentation (Sec 3.3) strategies, by comparison among GITA-7B trained on GVLQA-BASE and on the other augmentation subsets of GVLQA (Sec 4.2). Lastly, we investigate the effectiveness of using GVLQA as the pretrained dataset on real-world datasets. The evaluation metrics for all experiments are accuracy by exact matching. For the fine-tuning setting, we fine-tune the LoRA adapters (Hu et al., 2021) for all weight matrices within the text decoder of the VLM reasoner, while keeping the vision encoder in the VLM reasoner frozen. More detailed experimental settings are in Appendix F.

5.1 Evaluation on the GVLQA-BASE Dataset

In this subsection, we perform experiments on the GVLQA-BASE dataset by comparing GITA with popular LLMs-based baselines including GPT-4 Turbo (OpenAI, 2023), LLaMA2-7B/13B (Touvron et al., 2023), and Vicuna-7B/13B (Zheng et al., 2023), under both zero-shot and fine-tuning settings. The experimental results are shown in Table 1. From these results, we summarize the following observations.

Observation 1: GITA outperforms LLM Baselines. As can be seen in Table 1, GITA consistently outperforms the LLM baselines under the same setting. This underscores its SOTA effectiveness in instruction-based graph reasoning tasks, showing robust capabilities across different parameter scales under both fine-tuning and zero-shot settings. Moreover, under the fine-tuning setting, incorporating the vision modality consistently benefits 7B models. But for 13B models, the performance of some tasks may degrade. This could be attributed to the greater challenge of aligning the representation of visual and textual modalities in larger 13B models compared to 7B models, in the case of only fine-tuning LoRA adapters within the text decoder. We speculate that full training could potentially address this issue. However, we leave this as future work due to resource constraints.

Observation 2: Mainstream open-source VLM/LLMs lack fundamental graph reasoning abilities. The zero-shot results illustrate that prominent open-source LLMs or VLMs, including LLaMA2, Vicuna and LLaVA, exhibit minimal graph reasoning capabilities on the GVLQA-BASE dataset. Specifically, these models produce random answers, randomly responding with either "Yes." or "No." for tasks involving Connect and Cycle, resulting in a performance close to 50%. In contrast, current SOTA closed-source LLMs or VLMs, including GPT-4 Turbo and GPT-4V, demonstrate superior zero-shot performance compared to the aforementioned open-source models. This observation implies that current open-source LLMs and VLMs lack of basic graph reasoning ability, which may be attributed to the insufficient availability of relevant training data. Such observation also enhances the motivation for us to propose the GVLQA dataset, with the aim of improving the graph reasoning capabilities of VLMs/LLMs.

Observation 3: Model size increase enhances fine-tuning graph reasoning capabilities. The comparison of VLMs/LLMs with different parameter sizes, specifically 7B-parameter models and 13B-parameter models, highlights the benefits of increasing the model size for graph reasoning capabilities. In this regard, GITA-13B outperforms its counterpart with 7B parameters (GITA-7B) both on average and across four out of seven tasks. However, it is worth noting that GITA-13B does not outperform GITA-7B in the other three tasks. We hypothesize that this discrepancy may be attributed to insufficient modality alignment due to LoRA-only fine-tuning.

Observation 4: Vision and Text Modalities proficient in different types of Graph Reasoning Tasks. We explore the individual capabilities of the visual and textual modalities within the GITA framework. The results indicate that the text and vision modalities can complement each other and contribute to better performance than individual ones, as removing either modality leads to a drop in performance in most cases (Vicuna & GITA (VO) and GPT-4 Turbo & GITA (VO) in Table 1). While the graph reasoning capability provided by the vision may not be as strong as that of the text modality in most cases, relying solely on vision still enables the model to possess basic graph reasoning abilities. Specifically, the model outperforms text-based LLMs in 2/7 tasks (Cycle and BGM) when relying solely on vision. This consistent improvement across all comparison groups demonstrates the potential of the vision modality to excel in certain graph reasoning tasks, leveraging its ability to capture visual patterns like cycles and graph properties such as bipartition. In contrast, text exhibits a higher proficiency than vision modality in sequence-related graph reasoning problems, particularly in tasks like TS, SP, and HP, which require constructing ordered node sequences.

5.2 Evaluation for the Visual Graph Augmentations

To assess the impact of proposed visual graph augmentation strategies, including layout, node shape, node outline style, and edge thickness augmentations, we compare the performance of vision-only GITA-7B models trained on four augmented subsets of GVLQA and on GVLQA-BASE (without augmentation). The comparative results are presented in Table 2. To fully utilize the visual information in visual graphs, we fine-tune the visual encoder of VLMs in addition to the vision-to-text projector and the LoRA adapters within the text decoder in this part.

Table 2: Accuracy (%) comparisons across GVLQA subsets using GITA-7B (VO). \uparrow denotes dramatic performance improvement.

	Connect	Cycle	TS	SP	MaxFlow	BGM	HP	Avg
GVLQA-BASE	59.97	96.34	13.30	5.72	2.89	93.01	1.11	38.91
GVLQA-AUGNS	59.85	96.75	14.17	6.61	3.78	91.58	1.48	39.17
GVLQA-AUGNO	54.87	96.50	14.29	5.54	3.94	92.83	1.11	38.44
GVLQA-AUGET	57.98	96.91	13.37	5.97	3.11	91.76	0.74	38.55
GVLQA-AUGLY	87.18 \uparrow	97.07	14.86	76.55 \uparrow	3.94	93.19	70.74 \uparrow	63.36 \uparrow

Table 3: Accuracy (%) comparisons on real-world datasets under zero-shot and fine-tuning settings, where \ddagger indicates the usage of a checkpoint pretrained in the Cycle task of GVLQA-BASE.

Models	ca-GrQc	ca-HepTh	PolBlogs	Cora	CiteSeer	Avg
<i>Zero-shot</i>						
LLaMA2-7B	40.59	48.89	10.74	24.35	30.33	30.98
Vicuna-7B	41.35	50.00	8.72	26.94	29.13	31.22
GITA-7B	71.95	86.06	46.98	31.37	30.63	53.40
GITA-7B \ddagger	72.02	86.08	48.32	32.10	31.83	54.07
<i>Fine-tuning</i>						
LLaMA2-7B	76.57	89.06	80.54	83.76	73.27	80.64
Vicuna-7B	78.95	89.85	80.54	84.87	74.17	81.68
GITA-7B	79.70	91.13	84.56	85.24	75.07	83.14
GITA-7B (w/ AUGLY)	79.77	91.21	85.23	85.24	75.68	83.43
GITA-7B \ddagger	80.46	91.68	85.23	86.35	76.57	84.06

From the obtained results, a significant enhancement in overall performance is observed with the introduction of layout augmentation (GVLQA-AUGLY). The average performance improves remarkably from 38.91% to 63.36%. Notably, significant improvements were observed in SP (5.72% to 76.55%), HP (1.11% to 70.74%), and Connect (59.97% to 87.18%). These findings highlight the critical role of layout augmentation in the generation of visual graphs. In other words, this observation suggests the potential for creating larger-scale datasets for vision-language-based graph reasoning, which could significantly contribute to the advancement of this field. Conversely, the other three augmentations do not yield such substantial performance improvements, further emphasizing the importance of layout augmentation in vision-language-based reasoning.

5.3 Evaluation on the Real-World Datasets

In this section, we illustrate the effectiveness of GITA on the ca-GrQC Leskovec et al. (2007) and ca-HepTh Leskovec et al. (2007) datasets for the link prediction task, and on the PolBlog Adamic & Glance (2005), Cora Yang et al. (2016) and CiteSeer Yang et al. (2016) datasets for the node classification task. Table 5 in the appendix presents the statistics of those datasets, where graph data could involve thousands of nodes/edges, making it infeasible to feed the entire graph into the model. Consequently, we employ k -hop subgraph sampling discussed in Sec 3.2, specifically with $k = 2$, to satisfy the token length restriction of LLMs and visual graph scope effectively.

The experimental Results are shown in Table 3. The presented results have also verified the effectiveness of GITA and the proposed layout augmentation. Notably, we highlight the benefits of using GVLQA-BASE as pretrained dataset by comparing it with GITA-7b. Performance improvements of 0.67% and 0.92% were observed under zero-shot and fine-tuning settings, respectively. This underscores the potential application value of the proposed GVLQA dataset.

5.4 Case Study

In this section, we present representative examples of graph information provided in both visual and textual formats, which may offer some intuitive interpretations for our experimental results. Specifically, we highlight a case where the GITA-7B (VO) model outperforms its LLMs-based counterpart in Figure 2 (a), and its opposite scenario in Figure 2 (b).

The task depicted in Figure 2 (a) is cycle detection and the correct answer is ‘No’. This is successfully identified by the vision-only GITA-7B model, while the text-based Vicuna-7B fails to recognize it. In this instance, cycle patterns appear to be more readily recognizable in visual graphs, whereas text-based LLMs face the challenge of identifying cycles from disordered textual descriptions of edges, which could inherently involve greater complexity and more challenges.

On the other hand, the fixed layout of visual graphs presented in GVLQA-BASE may impede the visual encoder in identifying the shortest path between two nodes, although we have verified layout augmentation can greatly improve the graph reasoning abilities of models, as shown in Sec. 5.2. This limitation might arise from the confusion caused by the visual distance within an image, without considering the weights between the nodes. For instance, in Figure 2(b), the correct answer is ‘4->6->0’, which visually appears as a more convoluted path but numerically has a shorter path length of $3 = 1 + 2$. In contrast, the incorrect answer given by GITA-7B (vision-only) is ‘4->2->0’, which has a higher path length cost of $4 = 1 + 3$ but visually seems like a more direct shortcut. This observation further validates the effectiveness of employing layout augmentation to enhance performance in this task. Layout variations of visual graphs play a crucial role in mitigating the visual confusion caused by the spatial arrangement within a visual graph. However, it seems more effective for text-based LLMs to handle explicitly separated nodes and weights, as illustrated in the red-highlighted text in Figure 2(b).

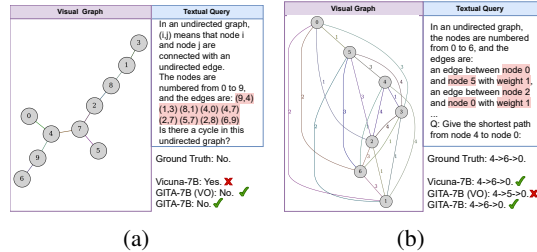


Figure 2: A comparative case study of graph representation in vision and text modalities. All methods are trained on the GVLQA-BASE dataset.

6 Conclusion

In this paper, we propose an end-to-end framework, called GITA, for vision-language-based graph reasoning. Our extensive experiments validate the superiority of incorporating visual information into instruction-based graph reasoning. Furthermore, we conduct a comparative analysis of the four proposed visual graph augmentations and identify layout augmentation as the most effective approach for enhancing visual graphs. This finding offers valuable insights for the development of larger-scale datasets aimed at facilitating vision-language-based graph reasoning. Lastly, we highlight the potential application value of the proposed GVLQA dataset as a pretrained dataset.

References

Adamic, L. A. and Glance, N. The political blogosphere and the 2004 us election: divided they blog. In *Proceedings of the 3rd international workshop on Link discovery*, pp. 36–43, 2005.

Alayrac, J.-B., Donahue, J., Luc, P., Miech, A., Barr, I., Hasson, Y., Lenc, K., Mensch, A., Millican, K., Reynolds, M., et al. Flamingo: a visual language model for few-shot learning. *Advances in Neural Information Processing Systems*, 35:23716–23736, 2022.

Andreas, J., Rohrbach, M., Darrell, T., and Klein, D. Neural module networks. In *Proceedings of the IEEE Conference on Computer Vision and Pattern Recognition*, pp. 39–48, 2016.

Battaglia, P., Pascanu, R., Lai, M., Jimenez Rezende, D., et al. Interaction networks for learning about objects, relations and physics. *Advances in neural information processing systems*, 29, 2016.

Battaglia, P. W., Hamrick, J. B., Bapst, V., Sanchez-Gonzalez, A., Zambaldi, V., Malinowski, M., Tacchetti, A., Raposo, D., Santoro, A., Faulkner, R., et al. Relational inductive biases, deep learning, and graph networks. *arXiv preprint arXiv:1806.01261*, 2018.

Bordes, A., Usunier, N., Garcia-Duran, A., Weston, J., and Yakhnenko, O. Translating embeddings for modeling multi-relational data. *Advances in neural information processing systems*, 26, 2013.

Cao, Q., Shen, H., Gao, J., Wei, B., and Cheng, X. Popularity prediction on social platforms with coupled graph neural networks. In *Proceedings of the 13th International Conference on Web Search and Data Mining*, pp. 70–78, 2020.

- Chen, D., O’Bray, L., and Borgwardt, K. Structure-aware transformer for graph representation learning. In *International Conference on Machine Learning*, pp. 3469–3489. PMLR, 2022.
- Chen, R., Zhao, T., Jaiswal, A., Shah, N., and Wang, Z. Llaga: Large language and graph assistant. *arXiv preprint arXiv:2402.08170*, 2024.
- Chen, Z., Mao, H., Li, H., Jin, W., Wen, H., Wei, X., Wang, S., Yin, D., Fan, W., Liu, H., et al. Exploring the potential of large language models (LLMs) in learning on graphs. *arXiv preprint arXiv:2307.03393*, 2023.
- Dai, W., Li, J., Li, D., Tiong, A., Zhao, J., Wang, W., Li, B., Fung, P., and Hoi, S. Instructblip: Towards general-purpose vision-language models with instruction tuning. *Advances in Neural Information Processing Systems*, 2023.
- Dantzig, G., Fulkerson, R., and Johnson, S. Solution of a large-scale traveling-salesman problem. *Journal of the operations research society of America*, 2(4):393–410, 1954.
- Dijkstra, E. W. A note on two problems in connexion with graphs. *Numerische Mathematik*, 1959.
- Fatemi, B., Halcrow, J., and Perozzi, B. Talk like a graph: Encoding graphs for large language models. In *Proceedings of International Conference on Learning Representations*, 2024.
- Ford, L. R. and Fulkerson, D. R. Maximal flow through a network. *Canadian Journal of Mathematics*, 1956.
- Gansner, E. R. and North, S. C. An open graph visualization system and its applications to software engineering. *Software: practice and experience*, 30(11):1203–1233, 2000.
- Gavin, A.-C., Aloy, P., Grandi, P., Krause, R., Boesche, M., Marzioch, M., Rau, C., Jensen, L. J., Bastuck, S., Dümpelfeld, B., et al. Proteome survey reveals modularity of the yeast cell machinery. *Nature*, 440(7084):631–636, 2006.
- Gilmer, J., Schoenholz, S. S., Riley, P. F., Vinyals, O., and Dahl, G. E. Neural message passing for quantum chemistry. In *International conference on machine learning*, pp. 1263–1272. PMLR, 2017.
- Gould, R. J. Advances on the hamiltonian problem—a survey. *Graphs and Combinatorics*, 2003.
- Guo, J., Du, L., and Liu, H. GPT4Graph: Can large language models understand graph structured data? an empirical evaluation and benchmarking. *arXiv preprint arXiv:2305.15066*, 2023.
- Hagberg, A., Swart, P., and S Chult, D. Exploring network structure, dynamics, and function using networkx. Technical report, Los Alamos National Lab.(LANL), Los Alamos, NM (United States), 2008.
- Hamilton, W., Ying, Z., and Leskovec, J. Inductive representation learning on large graphs. *Advances in neural information processing systems*, 30, 2017.
- He, X., Liao, L., Zhang, H., Nie, L., Hu, X., and Chua, T.-S. Neural collaborative filtering. In *Proceedings of the 26th international conference on world wide web*, pp. 173–182, 2017.
- He, X., Deng, K., Wang, X., Li, Y., Zhang, Y., and Wang, M. Lightgcn: Simplifying and powering graph convolution network for recommendation. In *Proceedings of the 43rd International ACM SIGIR conference on research and development in Information Retrieval*, pp. 639–648, 2020.
- He, X., Bresson, X., Laurent, T., Perold, A., LeCun, Y., and Hooi, B. Harnessing explanations: LLM-to-LM interpreter for enhanced text-attributed graph representation learning. In *Proceedings of International Conference on Learning Representations*, 2024.
- Hu, E. J., Wallis, P., Allen-Zhu, Z., Li, Y., Wang, S., Wang, L., Chen, W., et al. Lora: Low-rank adaptation of large language models. In *International Conference on Learning Representations*, 2021.

- Huang, C., Xu, H., Xu, Y., Dai, P., Xia, L., Lu, M., Bo, L., Xing, H., Lai, X., and Ye, Y. Knowledge-aware coupled graph neural network for social recommendation. In *Proceedings of the AAAI conference on artificial intelligence*, volume 35, pp. 4115–4122, 2021.
- Hudson, D. A. and Manning, C. D. Gqa: A new dataset for real-world visual reasoning and compositional question answering. In *Proceedings of the IEEE/CVF Conference on Computer Vision and Pattern Recognition*, pp. 6700–6709, 2019.
- Jeong, H., Mason, S. P., Barabási, A.-L., and Oltvai, Z. N. Lethality and centrality in protein networks. *Nature*, 411(6833):41–42, 2001.
- Johnson, J., Hariharan, B., Van Der Maaten, L., Fei-Fei, L., Lawrence Zitnick, C., and Girshick, R. Clevr: A diagnostic dataset for compositional language and elementary visual reasoning. In *Proceedings of the IEEE Conference on Computer Vision and Pattern Recognition*, pp. 2901–2910, 2017.
- Jui, T. D., Baker, E., and Benton, M. L. k-hopped link prediction with graph embedding. In *2023 Congress in Computer Science, Computer Engineering, & Applied Computing (CSCE)*, pp. 600–607. IEEE, 2023.
- Kahn, A. B. Topological sorting of large networks. *Communications of ACM*, 1962.
- Karp, R. M., Vazirani, U. V., and Vazirani, V. V. An optimal algorithm for on-line bipartite matching. In *Proceedings of the twenty-second annual ACM symposium on Theory of computing*, 1990.
- Kipf, T. N. and Welling, M. Semi-supervised classification with graph convolutional networks. *arXiv preprint arXiv:1609.02907*, 2016.
- Koren, Y., Bell, R., and Volinsky, C. Matrix factorization techniques for recommender systems. *Computer*, 42(8):30–37, 2009.
- Kreuzer, D., Beaini, D., Hamilton, W., Létourneau, V., and Tossou, P. Rethinking graph transformers with spectral attention. *Advances in Neural Information Processing Systems*, 34:21618–21629, 2021.
- Leskovec, J., Kleinberg, J., and Faloutsos, C. Graph evolution: Densification and shrinking diameters. *ACM transactions on Knowledge Discovery from Data (TKDD)*, 1(1):2–es, 2007.
- Leskovec, J., Backstrom, L., Kumar, R., and Tomkins, A. Microscopic evolution of social networks. In *Proceedings of the 14th ACM SIGKDD international conference on Knowledge discovery and data mining*, pp. 462–470, 2008.
- Li, J., Li, D., Savarese, S., and Hoi, S. BLIP-2: bootstrapping language-image pre-training with frozen image encoders and large language models. In *International conference on machine learning*, 2023.
- Liu, C. and Wu, B. Evaluating large language models on graphs: Performance insights and comparative analysis. *arXiv preprint arXiv:2308.11224*, 2023.
- Liu, H., Li, C., Wu, Q., and Lee, Y. J. Visual instruction tuning. *Advances in Neural Information Processing Systems*, 2023.
- Liu, X., Zhao, S., Su, K., Cen, Y., Qiu, J., Zhang, M., Wu, W., Dong, Y., and Tang, J. Mask and reason: Pre-training knowledge graph transformers for complex logical queries. In *Proceedings of the 28th ACM SIGKDD Conference on Knowledge Discovery and Data Mining*, pp. 1120–1130, 2022.
- Newman, M. E. The structure and function of complex networks. *SIAM review*, 45(2):167–256, 2003.
- OpenAI. GPT-3.5. Technical report, 2022.
- OpenAI. GPT-4 Turbo. Technical report, 2023.

- Perozzi, B., Fatemi, B., Zelle, D., Tsitsulin, A., Kazemi, M., Al-Rfou, R., and Halcrow, J. Let your graph do the talking: Encoding structured data for llms. *arXiv preprint arXiv:2402.05862*, 2024.
- Radford, A., Kim, J. W., Hallacy, C., Ramesh, A., Goh, G., Agarwal, S., Sastry, G., Askell, A., Mishkin, P., Clark, J., et al. Learning transferable visual models from natural language supervision. In *International conference on machine learning*, pp. 8748–8763. PMLR, 2021.
- Sedgewick, R. *Algorithms in C, part 5: graph algorithms*. Pearson Education, 2001.
- Socher, R., Chen, D., Manning, C. D., and Ng, A. Reasoning with neural tensor networks for knowledge base completion. *Advances in neural information processing systems*, 26, 2013.
- Suhr, A., Zhou, S., Zhang, A., Zhang, I., Bai, H., and Artzi, Y. A corpus for reasoning about natural language grounded in photographs. In *Proceedings of the 57th Annual Meeting of the Association for Computational Linguistics*, pp. 6418–6428, 2019.
- Tang, J., Yang, Y., Wei, W., Shi, L., Su, L., Cheng, S., Yin, D., and Huang, C. Graphgpt: Graph instruction tuning for large language models. *arXiv preprint arXiv:2310.13023*, 2023.
- Tosi, S. *Matplotlib for Python developers*. Packt Publishing Ltd, 2009.
- Touvron, H., Martin, L., Stone, K., Albert, P., Almahairi, A., Babaei, Y., Bashlykov, N., Batra, S., Bhargava, P., Bhosale, S., et al. Llama 2: Open foundation and fine-tuned chat models. *arXiv preprint arXiv:2307.09288*, 2023.
- Velickovic, P., Cucurull, G., Casanova, A., Romero, A., Lio, P., Bengio, Y., et al. Graph attention networks. *stat*, 1050(20):10–48550, 2017.
- Wang, H., Feng, S., He, T., Tan, Z., Han, X., and Tsvetkov, Y. Can language models solve graph problems in natural language? In *NeurIPS*, 2023.
- Wang, X., Huang, T., Wang, D., Yuan, Y., Liu, Z., He, X., and Chua, T.-S. Learning intents behind interactions with knowledge graph for recommendation. In *Proceedings of the web conference 2021*, pp. 878–887, 2021.
- Wei, J., Wang, X., Schuurmans, D., Bosma, M., Ichter, B., Xia, F., Chi, E. H., Le, Q. V., and Zhou, D. Chain of thought prompting elicits reasoning in large language models. In *Proceedings of Neural Information Processing Systems*, 2022.
- Wu, Z., Pan, S., Chen, F., Long, G., Zhang, C., and Yu, P. S. A comprehensive survey on graph neural networks. *IEEE Transactions on Neural Networks and Learning Systems*, 2020.
- Xu, K., Hu, W., Leskovec, J., and Jegelka, S. How powerful are graph neural networks? *arXiv preprint arXiv:1810.00826*, 2018.
- Yang, Z., Cohen, W., and Salakhudinov, R. Revisiting semi-supervised learning with graph embeddings. In *International conference on machine learning*, pp. 40–48. PMLR, 2016.
- Ye, R., Zhang, C., Wang, R., Xu, S., and Zhang, Y. Natural language is all a graph needs. *arXiv preprint arXiv:2308.07134*, 2023.
- Yu, L., Jiang, W., Shi, H., Yu, J., Liu, Z., Zhang, Y., Kwok, J. T., Li, Z., Weller, A., and Liu, W. MetaMath: Bootstrap your own mathematical questions for large language models. In *Proceedings of International Conference on Learning Representations*, 2024.
- Zellers, R., Bisk, Y., Farhadi, A., and Choi, Y. From recognition to cognition: Visual common-sense reasoning. In *Proceedings of the IEEE/CVF Conference on Computer Vision and Pattern Recognition*, pp. 6720–6731, 2019.
- Zhang, C., Gao, F., Jia, B., Zhu, Y., and Zhu, S.-C. Raven: A dataset for relational and analogical visual reasoning. In *Proceedings of the IEEE/CVF Conference on Computer Vision and Pattern Recognition*, pp. 5317–5327, 2019.
- Zhang, D., Yu, Y., Li, C., Dong, J., Su, D., Chu, C., and Yu, D. Mm-llms: Recent advances in multimodal large language models. *arXiv preprint arXiv:2401.13601*, 2024.

- Zhang, J., Zhang, H., Xia, C., and Sun, L. Graph-bert: Only attention is needed for learning graph representations. *arXiv preprint arXiv:2001.05140*, 2020.
- Zhang, Z., Wang, J., Chen, J., Ji, S., and Wu, F. Cone: Cone embeddings for multi-hop reasoning over knowledge graphs. *Advances in Neural Information Processing Systems*, 34:19172–19183, 2021.
- Zheng, L., Chiang, W.-L., Sheng, Y., Zhuang, S., Wu, Z., Zhuang, Y., Lin, Z., Li, Z., Li, D., Xing, E., Zhang, H., Gonzalez, J. E., and Stoica, I. Judging LLM-as-a-judge with MT-bench and chatbot arena. In *NeurIPS (Datasets and Benchmarks Track)*, 2023.
- Zhou, D., Schärli, N., Hou, L., Wei, J., Scales, N., Wang, X., Schuurmans, D., Cui, C., Bousquet, O., Le, Q. V., and Chi, E. H. Least-to-most prompting enables complex reasoning in large language models. In *Proceedings of International Conference on Learning Representations*, 2023.
- Zhu, D., Chen, J., Shen, X., Li, X., and Elhoseiny, M. Minigt-4: Enhancing vision-language understanding with advanced large language models. *arXiv preprint arXiv:2304.10592*, 2023.

A Characteristics of GITA

Generalizability. By effectively separating task specifications from graph structures and employing distinct components to manage them individually, GITA can be utilized to address a diverse set of graph reasoning tasks without necessitating alterations to its underlying architecture. In this way, when facing different types of tasks, the only adjustment required is to modify the instructions in the questioner without modifying other components.

Flexibility. The components of GITA offer a broad spectrum of choices: (i) The graph visualizer seamlessly integrates various graphic tools such as graphviz, matplotlib and networkx. (ii) The questioner can be either manual-template crafted or automatically generated by an agent. (iii) The VLM reasoner is compatible with almost all the existing VLMs. Such versatility empowers the implementation of GITA to be highly flexible.

User-friendliness. By utilizing existing VLM models as the reasoner, GITA inherits their language capabilities, allowing it to respond in natural languages.

Scalability on Large Graphs.

In real-world scenarios, the graphs can be very large. However, feeding the entire graph into the language model is not feasible due to the limited context length of text tokens. Additionally, visually representing such large graphs can lead to congestion and difficult to interpret. To address those challenges and maintain the usability for both text and visual inputs, GITA samples subgraphs around the target nodes or links within k hops (Sec 3.2). This has been commonly used in graph-based learning Kipf & Welling (2016); Hamilton et al. (2017); Xu et al. (2018); Jui et al. (2023); Velickovic et al. (2017); Chen et al. (2022), and ensures efficiency without compromising usability.

B Datasets Statistics

Table 4: Statistics of the GVLQA dataset.

Subset	Connect	Cycle	TS	SP	MaxFlow	BMG	HP	Total
BASE	16,410	4,100	2,910	1,560	1,500	1,860	900	29,240
AUGLY	98,460	24,600	17,460	9,360	9,000	11,160	5,400	175,440
AUGNS	49,230	12,300	8,730	4,680	4,500	5,580	2,700	87,720
AUGNO	65,640	16,400	11,640	6,240	6,000	7,440	3,600	116,960
AUGET	65,640	16,400	11,640	6,240	6,000	7,440	3,600	116,960
Total	295,380	73,800	52,380	28,080	27,000	33,480	16,200	526,320

Table 5: Statistics of real-world datasets

	ca-GrQC	ca-HepTh	PolBlogs	Cora	CiteSeer
# Nodes	5,242	9,877	1,490	2,708	3,327
# Edges	14,496	25,998	19,025	5,278	4,676
domain	collaboration	collaboration	social	citation	citation
average degree	5.53	5.26	25.54	3.9	2.74

C Illustrations for Visualization Tools in Graph Visualizer

The GITA graph visualizer incorporates a variety of implementations for existing visualization tools such as Graphviz, Matplotlib with NetworkX, and igraph, each selected for their unique capabilities in graph rendering. These tools are implemented in our code as interchangeable modules, enhancing flexibility based on the requirements of different projects.

Figure 3 showcases some visual graphs produced by these different graph visualizer implementations.

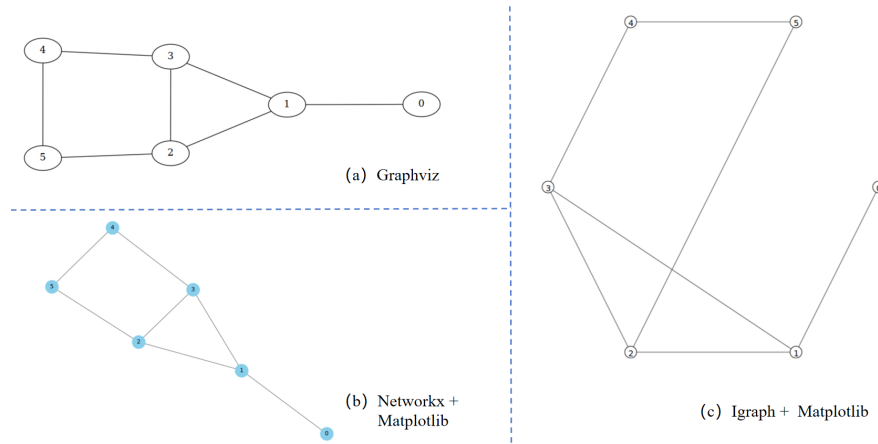


Figure 3: Examples of the visual graph generated by various visualization tools.

D Graph-describing Templates

The graph describer relies on a set of unified structured templates designed to generate coherent and informative descriptions that emphasize the inherent characteristics of the graph itself, regardless of specific task requirements. These graph-describing templates cover various scenarios, including directed graphs, undirected graphs, graphs with node identities or features, and graphs with edge weights or capacities. Table 6 provides an illustration of these templates, where [P] denotes placeholders required to be filled by corresponding graph information.

Graph categories	Undirected	Directed
Prototype	In an undirected graph, (i,j) means that node i and node j are connected with an undirected edge. The nodes are numbered from [P] to [P], and the edges are: $([P], [P]), ([P], [P])...$	In a directed graph, (i,j) means that node i and node j are connected with a directed edge from node i to node j . The nodes are numbered from [P] to [P], and the edges are: $([P], [P]), ([P], [P])...$
W/ Node Attributes	In an undirected graph, the nodes are numbered from [P] to [P], and every node has an attribute. (i,j) means that node i and node j are connected with an undirected edge. The attributes of nodes are: node [P]: [P] node [P]: [P] ... The edges are: $([P],[P]) ([P],[P]) ...$	In a directed graph, the nodes are numbered from [P] to [P], and every node has an attribute. (i,j) means that node i and node j are connected with a directed edge from node i to node j . The attributes of nodes are: node [P]: [P] node [P]: [P] ... The edges are: $([P],[P]) ([P],[P]) ...$
W/ Edge Weights	In an undirected graph, the nodes are numbered from [P] to [P], and the edges are: an edge between node [P] and node [P] with weight [P], an edge between node [P] and node [P] with weight [P], ...	In a directed graph, the nodes are numbered from [P] to [P], and the edges are: an edge from node [P] to node [P] with weight [P], an edge from node [P] to node [P] with weight [P], ...
W/ Both	In an undirected graph, the nodes are numbered from [P] to [P], and every node has an attribute. The attributes of nodes are: node [P]: [P] node [P]: [P] ... And the edges are: an edge between node [P] and node [P] with weight [P], an edge between node [P] and node [P] with weight [P], ...	In a directed graph, the nodes are numbered from [P] to [P], and every node has an attribute. The attributes of nodes are: node [P]: [P] node [P]: [P] ... And the edges are: an edge from node [P] to node [P] with weight [P], an edge from node [P] to node [P] with weight [P], ...

Table 6: Graph-describing Templates for various categories.

E Examples of Manual-template-based and LLM-agent-bootstrapped Query Generation

Manual-template-based Query Generation. The queries Q_G^T can be generated by task-specific manual templates. These templates are manually crafted by human to supplement descriptions/instructions about 1) concrete meanings of nodes and edges, 2) task responsibilities and 3) input/output specifications into the task-agnostic graph description D_G . Therefore, the **precision** and **faith** of generated task-specific queries Q_G^T are guaranteed by human calibrations. An example of manual-template-based query generation for topological sorting is illustrated in Figure 4. In this example, placeholders [P] are used to represent information that scripts will automatically fill in.

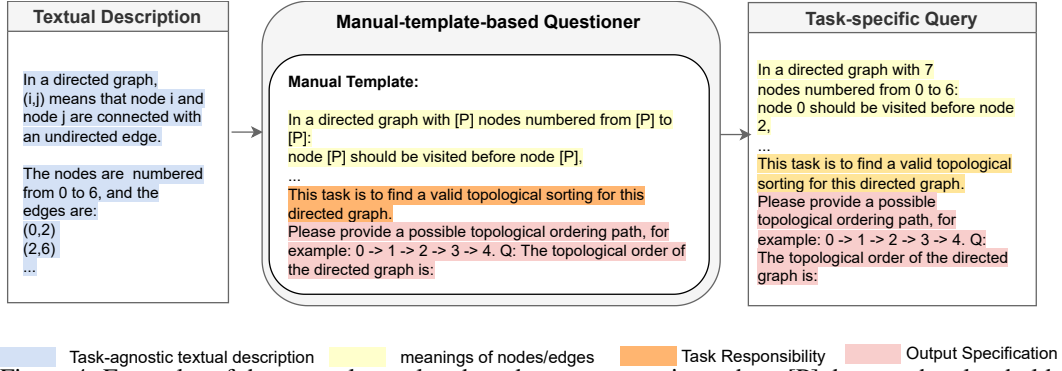


Figure 4: Examples of the manual-template-based query generation, where [P] denotes the placeholders.

LLM-agent-bootstrapped Query Generation. Figure 5 presents an example of employing a bootstrapped LLM agent, such as ChatGPT(OpenAI, 2022), for monster-hunting gaming. By incorporating task-specific information into the prompt, including node/edge meanings and task responsibilities, the LLM agent automatically generates a response that serves as the desired task-specific query. Compared to using manual templates, bootstrapping LLM agents for automated synthesis is more **flexible** and **economic** as it can take advantage of LLM agents to automatically interpret context and generate appropriate queries for various scenarios and minimize manual effort with changing conditions. Such properties make it suitable for dynamic or bespoke tasks, such as robotic planning or complex gaming scenarios.

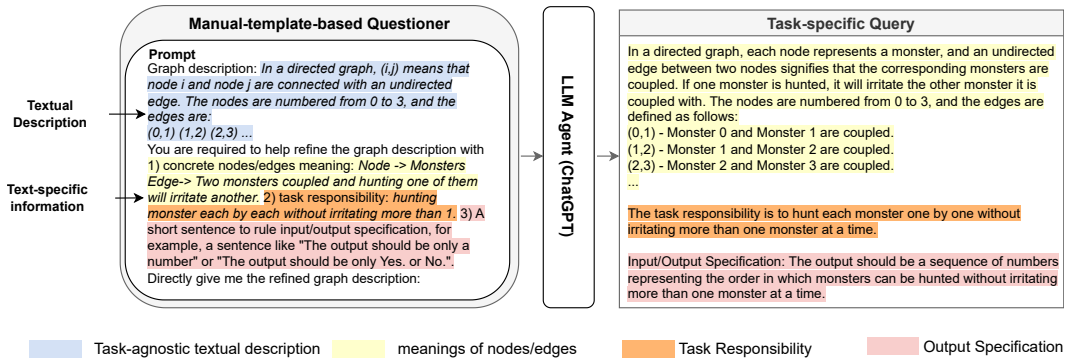


Figure 5: Examples of the LLM-agent-bootstrapped query generation.

F Experiment Settings

For all fine-tuning experiments, we use a batch size of 128 and adopt the AdamW optimizer (with a learning rate of 0.0002 and 0.00002 for the LoRA adapters within the text decoder and vision-to-text projector, respectively).

Detailed Settings for GVLQA Dataset During the evaluation, the temperature is set to 0 for all baselines. All fine-tuning experiments are conducted on an NVIDIA DGX station with 8xA100 GPUs. We split the GVLQA dataset in the ratio of 7:3 for training and testing, respectively. The accuracy (%) metrics are computed by comparing the prediction and ground truths with exact matching. We use the next-token-prediction loss to fine-tune the LoRA (Hu et al., 2021) adapters of LLMs and the vision-to-text projector. Visual graphs are encoded as visual embeddings by a visual encoder. Visual embeddings are concatenated with the embeddings of textual descriptions and instructions (i.e., questions), then fed to the text decoder to generate the answer.

Real-world Datasets Here we provide more details about the five real-world datasets used in Sec 5.3. The datasets ca-GrQC and ca-HepTh represent collaboration networks from the arXiv sections of General Relativity and Quantum Cosmology, and High Energy Physics - Theory, respectively, featuring nodes as authors and edges as co-authorships. They can be downloaded from Stanford Network Analysis Project (SNAP) website ³. PolBlogs is a network of U.S. political blogs from February 2005, categorized by political alignment and linked by blog references. Cora and CiteSeer are both citation networks, where nodes correspond to scientific papers and edges to citations, utilized for tasks such as document classification and citation analysis, with papers categorized into various research fields. Statistics of the datasets are shown in Table 5. For each dataset, 80%/10%/10% of the edges are randomly used for training/validation/testing, respectively.

Detailed Settings for Real-world Benchmarks In the conventional semi-supervised node classification setting, class labels are available for some nodes, which is reflected in the visual graph by coloring the nodes with a unique random color for each class. To focus on evaluating the model’s ability to capture structural information, GITA filters out the influence of node features in Cora and CiteSeer datasets. For link prediction tasks on ca-GrQC and ca-HepTh datasets, GITA treats the graphs as undirected. In the test split, both the original links and their reverse links do not appear in the train and valid splits. During training and evaluation, an equal number of negative sampled links are used alongside the positive links. These negative links are sampled at each training epoch but remain fixed during evaluation. For the GVLQA pretrain checkpoint, GITA adopts the 7B cycle checkpoint finetuned on GVLQA-BASE, where the performance is nearly mature. Hyperparameter combinations for each model are determined through grid search, and the specific combinations can be found in the provided code.

G Illustrations of GVLQA subsets

In this section, we present the illustrations of the GVLQA subsets. Figure 6 provides an overview of GVLQA-BASE. Subsequently, from Figure 7 to Figure 10, we showcase the augmented visual graphs in GVLQA-AUGLY (augment layouts), GVLQA-AUGNS (augment node styles), GVLQA-AUGNO (augment node outline styles), and GVLQA-AUGET (augment edge thickness), respectively.

H Limitation

The GITA framework proposed in the paper, along with its experimental results, exhibits certain limitations that should be acknowledged. Firstly, when dealing with large-scale graphs, the conventional subgraph sampling strategy employed by GITA may result in imbalanced and insufficient sampling, leading to the loss of critical graph structural information. This compromise is necessary to accommodate the limited contextual length of the text-based LLM and the restricted scope of the visual graph. Secondly, due to computational constraints, the fine-tuning procedures in the paper were restricted to the LoRA framework. While this approach offers advantages, a more comprehensive fine-tuning process that considers both visual and text modalities is expected to better align the two and potentially enhance performance. Addressing these limitations should be considered as a future research direction in this field.

³<https://snap.stanford.edu/index.html>

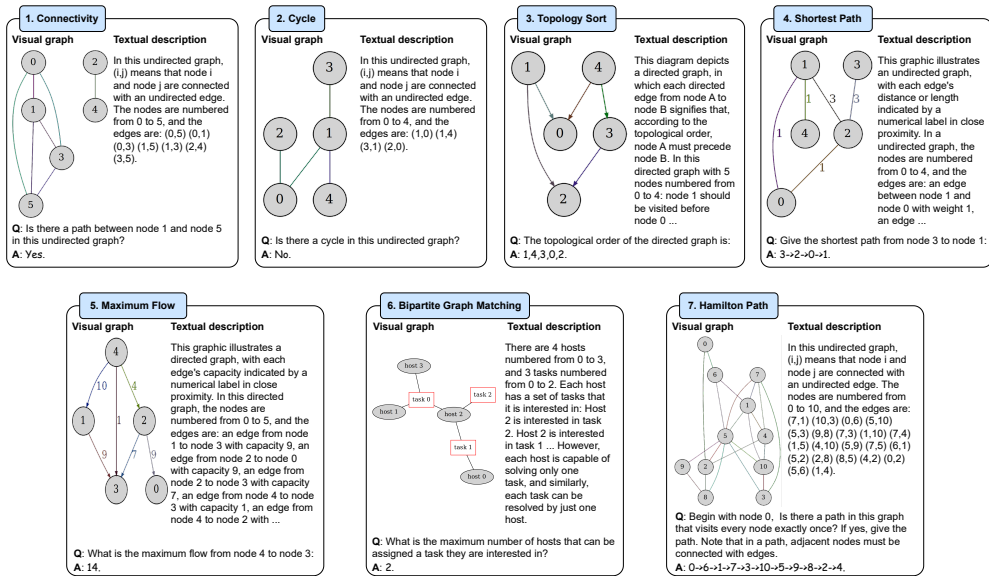


Figure 6: An overview of the GVLQA-BASE. Each figure depicts the tasks involving graph-based reasoning, showcasing a visual graph, a textual question, and the corresponding answer.

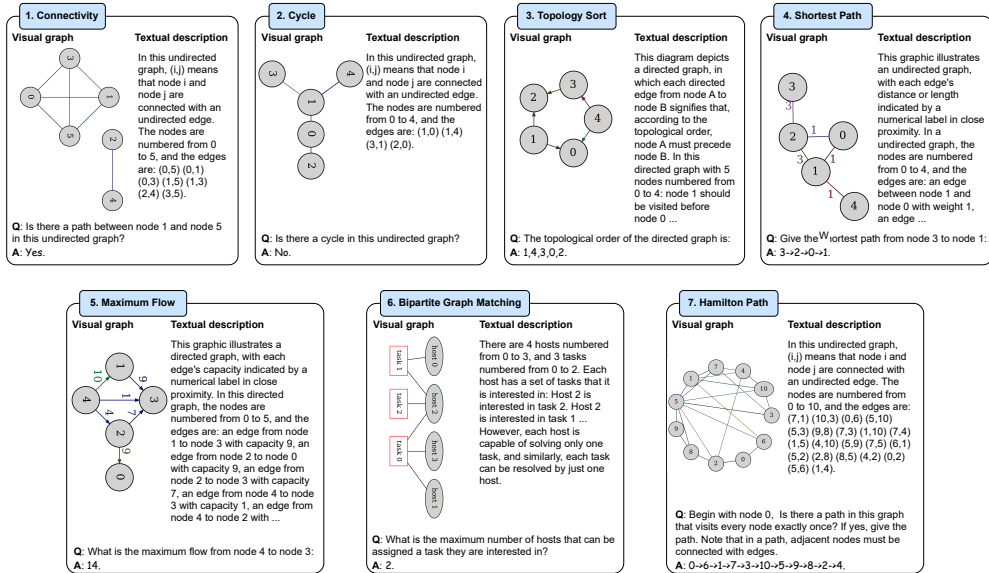


Figure 7: An overview of the GVLQA-AUGLY. Figures are akin to GVLQA-BASE but vary only in layouts.

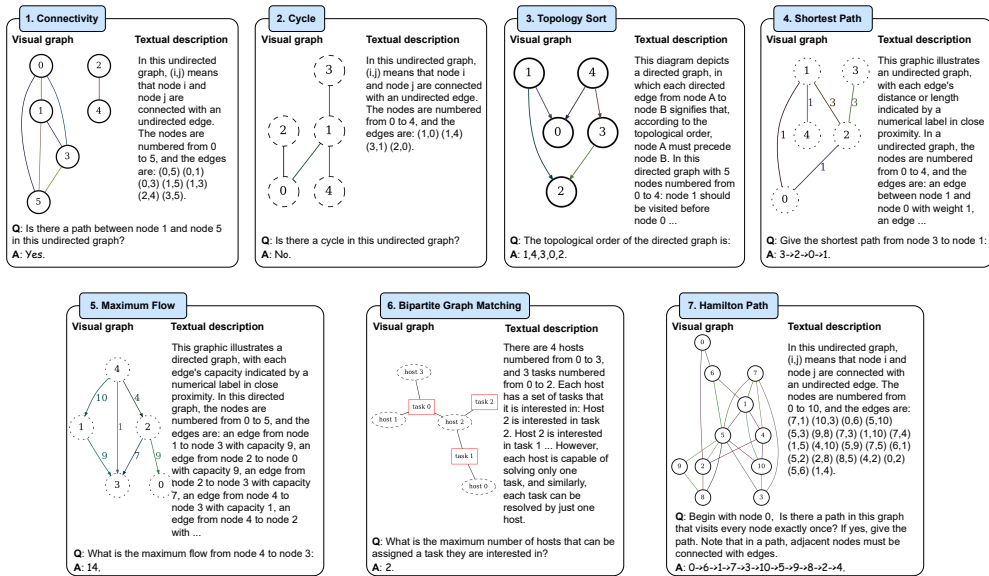


Figure 8: An overview of the GVLQA-AUGNO. Figures are akin to GVLQA-BASE but vary only in node outline styles.

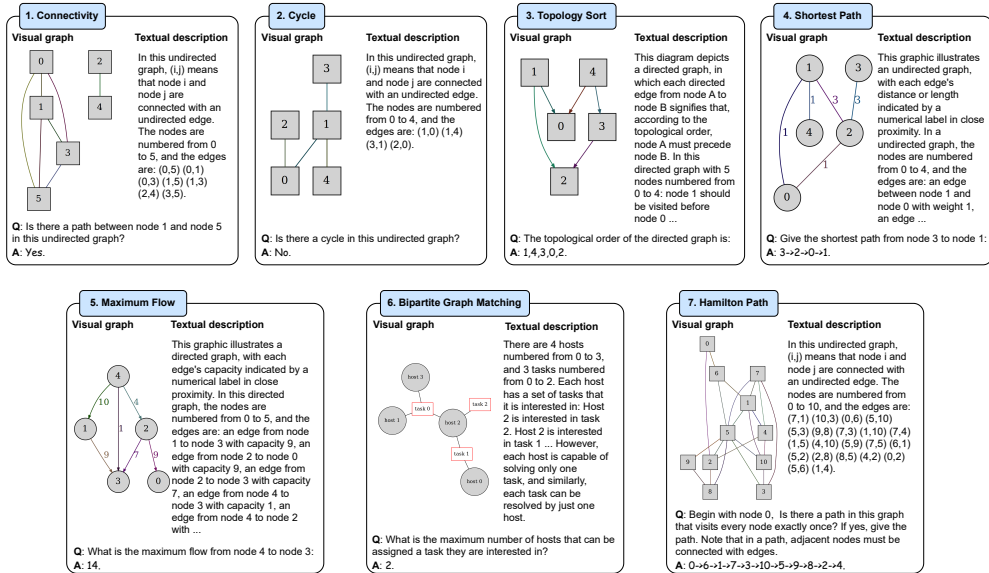


Figure 9: An overview of the GVLQA-AUGNS. Figures are akin to GVLQA-BASE but vary only in node shapes.

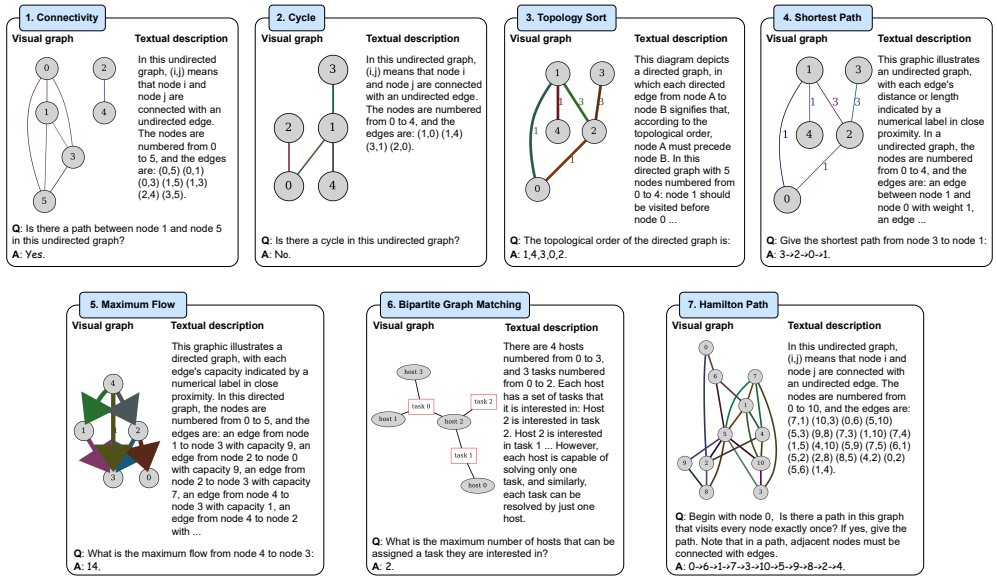


Figure 10: An overview of the GVLQA-AUGET. Figures are akin to GVLQA-BASE but vary only in edge thicknesses.